0026-895X/00/020359-08$3.00/0

MOLECULAR PHARMACOLOGY, **57**:359–366 (2000).

Drug-Resistant Variants of *Escherichia coli* Thymidylate Synthase: Effects of Substitutions at Pro-254

CORINNE FANTZ, DAVID SHAW, WILLIAM JENNINGS, ANTONIA FORSTHOEFEL, MARIA KITCHENS, JASON PHAN, WLADEK MINOR, LUKASZ LEBIODA, FRANKLIN G. BERGER, and H. TRENT SPENCER

Departments of Biological Sciences (D.S., W.J., A.F., M.K., F.G.B., H.T.S.) and Chemistry and Biochemistry (C.F., J.P., L.L.), University of South Carolina and the South Carolina Cancer Center (H.T.S.), Columbia, South Carolina; and Department of Molecular Pharmacology and Biophysics (W.M.), University of Virginia, Charlottesville, Virginia

Received February 1, 1999; accepted September 9, 1999

This paper is available online at http://www.molpharm.org

ABSTRACT

Drug-resistant variants of thymidylate synthase (TS) can potentially be used in gene therapy applications to decrease the myelosuppressive side effects of TS-directed anticancer agents or to select genetically modified cells in vivo. Mutations of proline 303 of human TS confer resistance to TS-directed fluoropyrimidines and antifolates (Kitchens et al., 1999). We generated the corresponding variants in *Escherichia coli* TS (ecTS), position 254, to better understand the mechanism by which mutations at this residue confer resistance. In addition, because ecTS is intrinsically resistant to several antifolates when compared with human TS, we suspected that greater resistance could be achieved with the bacterial enzyme. The P254L enzyme conferred >100-fold resistance to both raltitrexed and 5-fluoro-2′-deoxyuridine (FdUrd) compared with wild-type ecTS. Four additional mutants (P254F, P254S, P254G, and P254D), each of which complemented growth of a TS-deficient cell line, were generated, isolated, and characterized. Steady-state values of K_m for dUMP and k_{cat} were not substantially different among the variants and were comparable with the wild-type values, but K_m for methylenetetrahydrofolate (CH_2H_4PteGlu) was >10-fold higher for P254D. Values of k_{on} and k_{off} for nucleotide binding, which were obtained by stopped-flow spectroscopy, were virtually unchanged among the mutants. Drastic differences were observed for CH_2H_4PteGlu binding, with K_d values >15-fold higher than observed with the wild-type enzyme; surprisingly, the proposed isomerization reaction that is very evident for the wild-type enzyme is not observed with P254S. The decrease in affinity for CH_2H_4PteGlu correlates well with K_i values obtained for three TS-directed inhibitors. These results show that mutations at Pro-254 specifically affect the initial binding interactions between enzyme and cofactor and also alter the ability of the mutant enzymes to undergo conformational changes that occur on ternary complex formation. The crystal structure of P254S was determined at 1.5 Å resolution and is the most precise structure of TS available. When compared with wild-type TS, the structure shows local conformational changes affecting mostly Asp-253; its carbonyl is rotated approximately 40°, and the side chain forms an ion pair with Arg-225.

Effective drug treatment of human malignancies can be hampered by myelosuppressive side effects that result in increased susceptibility to life-threatening infections. The understanding of the molecular events leading to drug resistance has allowed investigators to test the feasibility of transferring genes that confer such resistance into normal cells. Gene transfer of chemoprotecting genes into bone marrow cells has the potential of protecting multiple hematopoietic lineages from the deleterious effects of chemotherapy, thereby allowing more aggressive chemotherapeutic dosing (reviewed in Koc et al., 1996). In addition to attenuating myelosuppression, genes that confer chemoprotection can provide a selective advantage to genetically modified hematopoietic cells. Studies using gene transfer of the cDNA that encodes MDR-1 or dihydrofolate reductase (DHFR) provide evidence that selectable markers can be used for in vivo enrichment of gene-modified cells (Sorrentino et al., 1992; Spencer et al., 1996; Allay et al., 1998).

Although the use of MDR-1 and DHFR have advanced to clinical trials (Hesdorffer et al., 1994; O'Shaughnessy et al., 1994; Deisseroth et al., 1996), there is a need to adapt such technologies to the attenuation of side effects of other important neoplastic agents. Thymidylate synthase (TS) is an excellent candidate for drug-resistant gene therapy, because it is a pre-eminent target for the design of new anticancer agents [e.g., raltitrexed (Tomudex) and BW1843U89]. In addition, it is the target of mainstream chemotherapy agents (e.g., 5-FU); the recombinant enzyme has been well-characterized, and the cDNA that encodes TS is relatively small

[1] This work was supported by Grants CA 78651 and CA 76560 from the National Cancer Institutes.

ABBREVIATIONS: DHFR, dihydrofolate reductase; TS, thymidylate synthase; ecTS, *Escherichia coli* TS; CH_2H_4PteGlu, methylenetetrahydrofolate; PCR, polymerase chain reaction; FdUrd, 5-fluoro-2′-deoxyuridine; MES, 2-(*N*-morpholino)ethanesulfonic acid.

(<1,000 base pairs) (Davisson et al., 1989; Carreras and Santi, 1995; Reilly et al., 1995; Touroutoglou and Pazdur, 1996; Spencer et al., 1997).

TS catalyzes the transfer of a methyl group from methylenetetrahydrofolate (CH_2H_4PteGlu) to dUMP, forming TMP. Inhibition of TS results in apoptotic cell death that is caused by intracellular thymidine depletion. Acquired resistance to TS inhibitors is a multifactorial process that can include amplification and/or mutation of the TS gene. In cells adapted to high concentrations of FdUrd, we showed that TS gene amplification in addition to mRNA and enzyme overproduction were commonly observed (Kitchens et al., 1999). For some adapted cell lines, overproduction of mRNA and protein were discordant, indicating that post-transcriptional mechanisms are involved in the resistance phenotype. A Pro to Leu substitution at residue 303 of human TS was identified and shown to be the effector of 5-fluoro-2′-deoxyuridine (FdUrd) resistance.

Crystal structures and rate constants governing individual steps in the catalytic mechanism of human TS are not available. Therefore, to better understand the mechanism by which mutations at residue 303 of human TS confer drug resistance, we generated the corresponding mutation in *Escherichia coli* TS (ecTS), which is structurally and kinetically well-characterized. In addition, because ecTS is intrinsically resistant to several TS-directed antifolates, it was anticipated that greater resistance could be achieved using the bacterial enzyme. Five amino acid substitutions were generated at residue 254, which is homologous to residue 303 of human TS, and steady-state and transient-state kinetic parameters were determined for each. The crystal structure of P254S TS was determined and used to explain its kinetic and mechanistic variations from the wild-type enzyme. The results show that mutations at Pro-254 decrease enzyme stability and decrease the affinity of the enzyme for CH_2H_4PteGlu and for three TS-directed antifolates but that the substitutions have little effect on nucleotide binding or the rate-limiting step of catalysis. The drastic decrease in antifolate affinity suggests that variants at residue 254 in ecTS may be suitable for use as drug-resistant markers in gene therapy applications.

Experimental Procedures

Site-Directed Mutagenesis and Growth Complementation Studies. The gene encoding ecTS, a gift from Dr. Dallas (Glaxo Wellcome, Research Triangle Park, NC), was amplified by polymerase chain reaction (PCR) to introduce *Xba*I and *Cla*I sites at the 5′- and 3′-ends of the coding region, respectively. The amplified sequence was cloned into the *Xba*I/*Cla*I sites of pBluescript SK (Stratagene, La Jolla, CA), which generated pBSecTS, transformed into XL-1 Blue bacterial cells, and sequenced to confirm the integrity of the ecTS gene. Mutations at residue 254 were produced by PCR mutagenesis using the overlap extension method to generate a 570-base pair product (Ho et al., 1989). The PCR product was digested with *Nsi*I and *Cla*I and cloned into the *Nsi*I/*Cla*I sites of pBSecTS. The entire cloned region was sequenced to confirm the presence of the mutation and assure the absence of undesired mutations.

Plasmids encoding wild-type ecTS or the Pro-254 mutated enzymes were transformed into the tetracycline-resistant, rec A-deficient, TS-deficient bacterial strain, χ2913. Transformed cells were grown in defined medium with tetracycline (selects for χ2913 cells) and ampicillin (selects for transformed cells) but which lacked thymidine (selects for active TS mutants).

Protein Purification. Cell free extracts were obtained from 2 g of wet cells by five 30-s consecutive sonication cycles (Branson Sonifier 450; Danbury, CT) in 25 ml of degassed QA buffer (50 mM Tris, 14 mM 2-mercaptoethanol, and 1 mM EDTA, pH 7.5), centrifuged at 11,000*g* for 30 min, and applied to a DEAE Affi-Gel Blue (Sigma, St. Louis, MO) column (2.5 × 15-cm) pre-equilibrated in QA buffer. The column was washed with three column volumes of QA buffer, two column volumes of 100 mM KCl, then by two column volumes of 200 mM KCl in QA buffer. Enzyme activity routinely eluted in 200 mM KCl. The eluted enzyme was dialyzed against QA buffer and applied to a 2.5 × 20-cm Q-Sepharose FPLC column (Amersham Pharmacia Biotech, Piscataway, NJ) that had been equilibrated with degassed QA buffer. Elution was accomplished by using a 500-ml linear gradient of 200 to 600 mM KCl in QA buffer. Fractions were monitored for TS activity, which typically eluted between 360 and 420 mM KCl. Enzyme purity was assessed by SDS polyacrylamide gel electrophoresis, and purified proteins were stored in 15% glycerol at −70°C.

Kinetic Characterization of ecTS and Pro-254 Variants—Steady-State Determinations. The concentration of purified enzymes was determined using a molar extinction coefficient at 280 nm of 1.13×10^5 M^{-1} cm^{-1}, and the number of binding sites was determined by FdUMP titration of protein absorbance at 330 nm. The concentrations of 1/2 binding sites were in good agreement with the concentrations determined by UV absorbance at 280 nm. The value of $K_{m(dUMP)}$ was determined using concentrations of dUMP between 1 and 100 μM with 100 μM CH_2H_4PteGlu, except 500 μM CH_2H_4PteGlu was used for P254D. The value of $K_{m(CH2H4PteGlu)}$ was determined using CH_2H_4PteGlu concentrations in the range of 6 to 300 μM in the presence of 100 μM dUMP. Reactions were performed at 20°C in 100 mM Tris-HCl (pH 7.4), 1 mM EDTA, and 14 mM 2-mercaptoethanol, and activity was followed by measuring the absorbance at 340 nm. Velocity values were plotted versus the concentration of ligand, and the values of K_m and k_{cat} were determined using the program KaleidaGraph (Synergy Software, Reading, PA). Values of K_i were determined using the program EZ-fit (Perrella Scientific, Amherst, NH) with enzyme concentrations ranging from 20 to 200 nM, dUMP concentrations of 100 μM, and CH_2H_4PteGlu concentrations 3 times the K_m values.

Kinetic Characterization of ecTS and Pro-254 Variants—Transient-State Determination. Ligand binding was followed on an Applied Photophysics (Surrey, UK) SX-18 stopped-flow fluorometer/spectrophotometer at 20°C in activation buffer (100 mM Tris buffer, pH 7.4, containing 10 mM 2-mercaptoethanol) using an excitation wavelength of 295 nm and emission wavelengths 330 nm as previously reported (Spencer et al., 1997). Enzymes and ligands were diluted in activation buffer to concentrations 2 times that indicated within the text or in figure legends. After collection, data were computer-fitted by nonlinear least-squares analysis to equations describing single or multiple exponential terms using KaleidaGraph 3.0.1. At least five traces were averaged for every ligand concentration. The entire experiment for the determination of the association and dissociation rate constants was repeated a minimum of two times for each mutant.

Survival Curves. The cDNAs that encode wild type and P254L were cloned into the *Sac*II/*Xho*I sites of the HaMSV retroviral vector (Sorrentino et al., 1992; Spencer et al., 1996) and transfected into the TS-deficient Chinese hamster lung cell line RJK88.13. Selection of transfected cells was accomplished by removing thymidine from the medium. Survival curves were generated by plating 40,000 cells/25-cm^2 flask with various concentrations of TS inhibitors. After 5 to 7 days, surviving cells were counted after trypan blue staining. At least three flasks were used for each concentration of drug.

Determination of Protein Levels—FdUMP Binding Assay. Extracts from Chinese hamster lung cells that contained ecTS constructs were prepared by sonication from two nearly confluent 100-mm dishes. Reaction mixtures contained, in 500 μl, 50 μg of cell free extract, 300 μM CH_2H_4PteGlu, 100 μl of Morrison buffer (120 mM Tris, 60 mM MES, 60 mM acetic acid, pH 7.2) and either 100 or

200 nM [^{3}H]FdUMP. Following 1 h of incubation at room temperature, 125 μl of 50% trichloroacetic acid was added and centrifuged at 13,000*g* for 5 min. The pellet was washed four times with 10% trichloroacetic acid and resuspended in 2 N NaOH, 50% ethanol and counted. Concentrations of TS are expressed as picomoles of FdUMP bound per milligram of protein.

Crystallization of P254S TS. The purified enzyme was dialyzed against a buffer containing 1 mM EDTA, 10 mM 2-mercaptoethanol, 100 mM ammonium sulfate, and 20 mM potassium phosphate at pH 7.5 for 72 h. Crystals were grown using the vapor diffusion method in the hanging drop setup. Typically, 5 μl of TS solution at 20 mg/ml was mixed with an equal volume of a precipitating well solution (58% saturated ammonium sulfate, 20 mM 2-mercaptoethanol, and 100 mM Tris-HCl, pH 8.8) and allowed to equilibrate with the well. Crystals appeared after 21 days and grew to the size of 0.4 mm within 1 week.

Crystallography. A crystal measuring approximately .4 × .4 mm was transferred to a cryoprotectant solution and flash-frozen in liquid nitrogen. The data were collected at the SBC line of Advanced Photon Source at Argonne National Laboratory (Argonne, IL) using X-rays of 0.9793 Å in wavelength. Two sets of data were collected at high and low resolution with a 3 × 3 CCD array detector, and were indexed, integrated, and scaled with the HKL 2000 suit of programs (Otwinowski and Minor, 1997). The strategy option was used for collecting all possible independent reflections with minimum radiation damage to the crystal. In the first pass, oscillation frames were collected to record the high resolution data. The second pass was used to remeasure reflections that suffered from intensity overflow during the first pass. The detailed collection strategy is summarized in Table 5. The structure of S167T mutant (unpublished data) with the appropriate amino acid sequence modifications was used as the starting model in molecular replacement using CCP4 software (Computational Collaborative Project, 1994), and the data were optimized with the CNS software (Brunger et al., 1998) using positional and temperature refinements. Electron density maps calculated with $2F_o - F_c$, and $F_o - F_c$ coefficients were inspected to introduce corrections manually to the model with the interactive graphics program CHAIN (Sack and Quiocho, 1997).

Results

Location of Pro-254. Pro-254 in ecTS is located at a bend 11 amino acids from the C-terminal isoleucine residue. Its side chain is not exposed to solvent but makes contact with the side chain of Arg-48. Figure 1 shows that the proline does not make direct contact with either bound nucleotide or folate (Hyatt et al., 1997). However, the residue is situated in the middle of the final bend that directs the C-terminal residues toward the active site. The C-terminal residues, particularly the final four residues, are known to be crucial for CH_2H_4PteGlu binding.

Resistance Conferred by the P254L Mutant of ecTS. Substitution of leucine for proline at residue 303 of human TS confers resistance to fluoropyrimidines and antifolates (Kitchens et al., 1999). To determine whether the homologous substitution in ecTS confers resistance, we engineered the corresponding mutation at residue 254 of ecTS. The cDNAs that encode wild-type ecTS or the P254L mutant were introduced into the HaMSV retroviral vector and transfected into the TS-deficient cell line RJK88.13. Both constructs complemented cell growth in media lacking thymidine, and transfected cells had similar levels of TS protein expression (1.2 pmol/mg of protein) as determined by radiolabeled FdUMP titrations and similar growth rates. Similar to human TS, but to a much greater extent, substitution of leucine for proline confers resistance to raltitrexed (>100-fold) and FdUrd (>500-fold) (Fig. 2), indicating that ecTS is more sensitive to the Pro to Leu substitution than is the human enzyme. Cells transfected with the wild-type or mutant constructs were equally sensitive to the DHFR directed inhibitors methotrexate and trimetrexate.

Purification of Pro-254 Variants. To determine the effects of amino acid substitutions at position 254, proline was substituted with residues that represent various classes of amino acids, including leucine, glycine, phenylalanine, serine, and aspartic acid. With the exception of leucine, all enzymes complemented the growth of TS-deficient χ2913 bacterial cells and constituted about 15% soluble protein. The P254L enzyme was not present in cell-free extracts but precipitated presumably into inclusion bodies; only inactive protein was recovered in the cell sonicates (data not shown). Wild-type and the remaining four variants were isolated to >90% purity. In vitro stability studies using 1 μM purified enzyme and 50 μM dUMP showed that, with the exception of glycine, the variants were less stable at 37°C than wild-type ecTS (data not shown). Whereas the half-life of wild-type ecTS was 90 min, the half-life of P254F, P254S, and P254D were approximately 50 min.

Steady-State Kinetic Constants. Values of K_m for dUMP and CH_2H_4PteGlu, k_{cat} and catalytic efficiencies (measured as k_{cat}/K_m) are shown in Table 1. The values for k_{cat} and $K_{m(dUMP)}$ are similar among the enzymes, with P254D having the greatest variance from the wild-type value for both k_{cat} and $K_{m(dUMP)}$, but only by factors of 1.5 and 2.8, respectively. P254G, P254F, and P254S enzymes have $K_{m(CH2H4PteGlu)}$ values similar to the wild-type enzyme, whereas that for the P254D enzyme is >10-fold higher. Although the catalytic efficiencies of P254G, P254F, and P254S are similar to the wild-type enzyme, the decrease in k_{cat} and increase in $K_{m(CH2H4PteGlu)}$ for P254D lowers the catalytic efficiency of this enzyme by approximately 15-fold.

Transient State Kinetic Constants—dUMP Binary Complex Formation. Because the values of K_m depend on several rate constants, specific values that govern individual

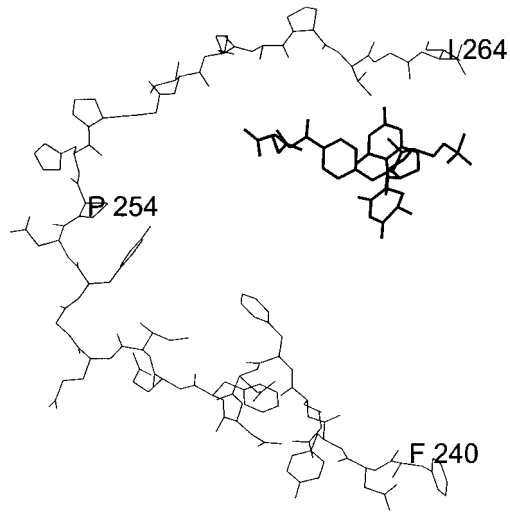

Fig. 1. Position of the 25 C-terminal residues of ecTS in a ternary complex with CH_2H_4PteGlu and FdUMP (bold lines). The position of proline 254 and the C-terminal isoleucine are indicated within the figure, which was obtained using coordinates from the Protein Data Bank file, access code 1tsn (Hyatt et al., 1997).

steps along the catalytic pathway were determined. For ecTS the binding of dUMP is a simple bimolecular association reaction opposed by a unimolecular dissociation reaction. The binding of dUMP causes quenching of intrinsic protein fluorescence, the rate of which can be used to determine k_{on} and k_{off} values using the relationship $k_{obs} = k_{on}$ [dUMP] + k_{off} (Spencer et al., 1997). Table 2 shows k_{on}, k_{off}, and K_d (as defined by k_{off}/k_{on}) values for the wild-type and P254F, P254S, and P254D enzymes. Because these values are not substantially different among the enzymes, these results show that nucleotide binding is not severely affected by the Pro-254 mutations.

Transient State Kinetic Constants—CH_2H_4PteGlu binding. It has been shown that binding of CH_2H_4PteGlu into the ternary complex of wild-type ecTS·dUMP can be described by Scheme 1, where L = CH_2H_4PteGlu and E = ecTS·dUMP and P = product of reaction (Spencer et al., 1997).

$$E + L \overset{K_d}{\rightleftharpoons} EL \underset{k_{r,iso}}{\overset{k_{iso}}{\rightleftharpoons}} EL^* \xrightarrow{k_{chem}} E + P$$

Scheme 1

K_d is the dissociation constant for the initial binding of CH_2H_4PteGlu, k_{iso} and $k_{r,iso}$ are the first-order rate constants governing the isomerization or interconversion of EL to EL^*, and k_{chem} is the rate constant governing the chemical conversion of substrates to products. On mixing of CH_2H_4PteGlu with ecTS · dUMP, a decrease in fluorescence is observed, the rate of which is hyperbolically dependent on the concentration of CH_2H_4PteGlu (Fig. 3). For wild-type ecTS, the dependence of the observed rate on CH_2H_4PteGlu concentration is described by $k_{obs} = k_{iso}[L]/(L + K_d) + k_{r,iso} + k_{chem}$ (Spencer et al., 1997), which allows for the determination of K_d, k_{iso}, $k_{r,iso}$ and k_{chem}, the values of which are reported in Table 3. Similar to wild-type ecTS, the dependence of k_{obs} on CH_2H_4PteGlu concentration is hyperbolic for P254F (data is omitted from Fig. 3 for clarity) but the affinity of the initial binding of CH_2H_4PteGlu is approximately 2-fold lower compared with wild-type ecTS and, because of a decrease in the rate governing the forward isomerization, almost 5-fold lower after protein isomerization (Table 3).

Interestingly, k_{obs} for P254S does not show the hyperbolic dependence on CH_2H_4PteGlu concentration, suggesting that the affinity of ligand is not increased after binding and that the isomerization reaction is not significant for this variant. The binding of CH_2H_4PteGlu to P254S can be described by a bimolecular association followed by a unimolecular dissociation. The dependence of k_{obs} on CH_2H_4PteGlu concentration can, therefore, be described by $k_{obs} = k_{on}$[CH_2H_4PteGlu] + k_{off} and K_d as k_{off}/k_{on} (Table 3). Similar to P254S, P254D does not appear to show hyperbolic dependence of k_{obs} on CH_2H_4PteGlu concentration. However, the K_d value for this variant is very high, and the curvature may not be apparent at the ligand concentrations used. Differences in the dependence of k_{obs} as a function of ligand concentration clearly indicate that substitutions at position 254 in ecTS affect cosubstrate binding as well as the ability of the variant enzymes to undergo isomerization after ligand binding.

Binary Complex Formation between FdUMP and Enzyme. Because a P303L mutation of human TS was identified in a FdUrd resistant cell line, rate constants governing FdUMP binary complex formation for the P254D enzyme were determined. Although the k_{on} and k_{off} values for dUMP

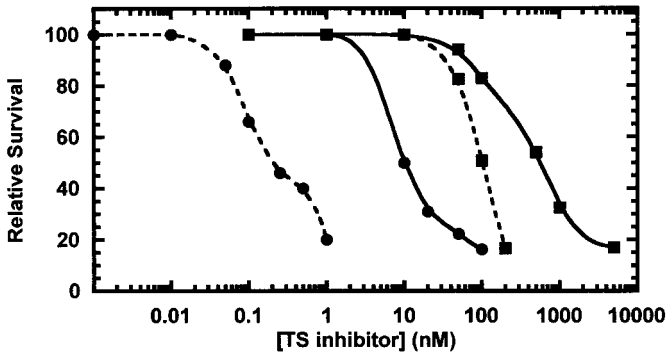

Fig. 2. Growth curves of TS-deficient cells transfected with wild-type (circles) or P254L ecTS (squares), selected in media lacking thymidine and grown in the presence of various concentrations of either FdUrd (dashed lines) or raltitrexed (solid lines).

TABLE 1

Steady-state kinetic constants for Pro-254 ecTS variants

All values were obtained in triplicate. The standard errors are <10% of the reported values.

Enzyme	k_{cat}	K_m (dUMP)[a]	K_m (CH_2H_4PteGlu)[b]	k_{cat}/K_m (dUMP)	k_{cat}/K_m (CH_2H_4PteGlu)
	s^{-1}	μM	μM		
WtecTS	2.1	1.2	11	1.8	0.19
P254G	2.0	1.5	12	1.3	0.17
P254F	1.8	1.8	18	1.0	0.10
P254S	1.9	2.7	10	0.70	0.19
P254D	1.5	3.4	118	0.44	0.013

[a] Determined in the presence of 100 μM CH_2H_4PteGlu except for P254D, which was determined in the presence of 500 μM CH_2H_4PteGlu.
[b] Determined in the presence of 100 μM dUMP.

TABLE 2

Kinetic parameters governing dUMP binary complex formation

Values were determined from the linear relationship of k_{obs} and dUMP concentration where $k_{obs} = k_{on}$[dUMP] + k_{off}. Values of k_{obs} were obtained by stopped-flow spectroscopy as described in *Experimental Procedures*. All values were obtained in triplicate. The standard errors are <10% of the reported values.

Enzyme	Wild-type ecTS	P254F	P254S	P254D
k_{on} (μM^{-1} s^{-1})	9.8	4.5	6.2	11
k_{off} (s^{-1})	41	33	43	45
K_d (μM)[a]	4.2	7.3	6.9	4.0

[a] Determined from $K_d = k_{off}/k_{on}$.

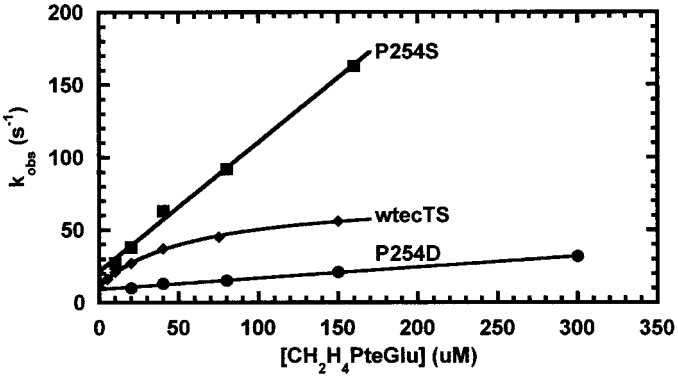

Fig. 3. Dependence of k_{obs} on the concentration of CH_2H_4PteGlu for wild-type (diamonds), P254S (squares), and P254D ecTS (circles). Final enzyme and dUMP concentrations were 2 and 500 μM, respectively. Refer to Table 3 for values obtained from the individual fits.

binding were not substantially affected by the mutations, the dissociation constant (K_d) for FdUMP is >3-fold higher (Table 4). The difference is mainly due to an increase in the value of k_{off} (Table 4). Compared with the binding of dUMP to P254D, FdUMP binds with >6-fold weaker affinity.

Transient State Kinetic Constants—AG337 binding. Many tight-binding antifolate-based inhibitors of TS have recently been developed. We used stopped-flow spectroscopy to determine the effects of Pro-254 substitutions on the binding of raltitrexed, BW1843U89, and AG337. Raltitrexed and BW1843U89 have high values of k_{on} (>60 μM^{-1} s^{-1}) and very low values of k_{off} (<5 s^{-1}). Because k_{off} is so low, it is impractical to compare the effects of Pro-254 mutations on the binding of these ligands. However, the initial binding of AG337 to wild-type ecTS has a k_{off} value of approximately 70 s^{-1}, allowing for an accurate comparison of the effects of Pro-254 mutations on the binding of an inhibitor that occupies the cofactor binding site.

On mixing AG337 with ecTS · dUMP, the intrinsic enzyme fluorescence is quenched. The rate of quenching is best described by a two-exponential equation. The observed rate of the first exponential is linearly dependent on ligand concentration, indicating that this process represents ligand binding. Values of k_{on} and k_{off} obtained from the linear fit of k_{obs} with the concentration of AG337 are shown in Table 4. The observed rate of the second exponential is not dependent on ligand concentration and has a value of approximately 40 s^{-1}, indicating that a conformational change occurs on AG337 binding. The binding of AG337 to the P254D enzyme is best described by a single exponential, and the observed rate of binding is linearly dependent on the concentration of AG337, which was used to calculate values of k_{on} and k_{off} (Table 4). The values of k_{on} for AG337 binding to wild-type ecTS and to the P254D enzyme are similar, but the value of k_{off} is approximately 7-fold higher for P254D, increasing the value of K_d >7-fold (Table 4).

Affinity of TS-Targeted Inhibitors and the Ability to Confer Drug Resistance. Compared with human TS, wild-type ecTS has higher K_i values for raltitrexed and AG337 but a similar K_i value for BW1843U89, which is consistent with previously reported results (Jackson et al., 1993). The P254S and P254F mutants and wild-type ecTS have similar K_i values for these three inhibitors. However, K_i values are drastically increased for P254D, the greatest increase is observed with raltitrexed (>10-fold compared with wild-type ecTS and >100-fold compared with human TS) (Fig. 4A). P254D was cloned into the HaMSV retroviral vector and transfected into the TS^- cell line RJK88.13, and transformants were selected by removing thymidine from the growth media. Compared with cells transfected with either human TS or wild-type ecTS at similar enzyme levels (1.5 ± 0.3 pmol bound FdUMP/mg of protein), P254D conferred the greatest resistance to raltitrexed (Fig. 4B).

Crystallographic Data Measurement and Refinement. Steady-state kinetic and thermodynamic properties of P254S are virtually unchanged when compared with the wild-type enzyme. However, this mutation appears to affect ligand-induced isomerization. In an effort to better understand the effects of this mutation, high resolution data were collected from crystals of P254S to 100% completion with a mosaic spread of 0.37° and an R_{symm} of 12%. The detailed collection strategy is summarized in Table 5. The completeness is also 100% in the highest resolution shell, 1.55 to 1.50, with 4008 reflections having $I > 2\sigma(I)$. The low resolution set was 96.7% complete to 2.10 Å with an R_{symm} of 10%. The data were merged after rejecting intensity-saturated and weak reflections to give a 99.9% complete set of data to 1.50 Å. Merging of the two data sets yielded an R_{merge} of 6.6 and 91.1% of the reflections having $I/\sigma(I) > 2$. After several rounds of refinement and modeling, the $2F_o - F_c$ electron density map was superb; it revealed holes in aromatic and proline rings, and a bulge of density for every carbonyl group. However, electron density was missing for a few side chains, especially residues 19–22 at the β-bend located between helix A and strand I, which are partially disordered. The data were refined to a final R-factor of 22% and has been deposited at the Protein Data Bank as entry 1qqq. Figure 5 shows that the effects of the P254S mutation are local and that the most significant difference between the wild-type enzyme and P254S is a 40° rotation of the carbonyl plane of Asp-253. An ion pair is then capable of forming between Asp-253 and Arg-225. Although the positioning of the final four C-terminal residues (261–264) of P254S is slightly shifted compared with the wild-type enzyme, residues 257–260 are virtually unchanged.

TABLE 3

Transient state kinetic parameters for $CH_2H_4PteGlu$ binding

All values were obtained in triplicate. The standard errors are <10% of the reported values with the exception of the value of $K_d(CH_2H_4PteGlu)$ for P254D, which is 18%.

	ecTS	P254F	P254S	P254D
$K_d(CH_2H_4PteGlu)$ (μM)	63[a,b] (8.7)[c]	122[c] (41)[d]	24[d]	150[d]
k_{iso} (s^{-1})	62[a]	8.5	n.o.[e]	n.o.[e]
k_{riso} (s^{-1})	10[a]	4.2	n.o.[e]	n.o.[e]
k_{on} (μM^{-1} s^{-1})	n.a.[f]	n.a.[f]	0.9	0.07
k_{off} (s^{-1})	n.a.[f]	n.a.[f]	21.4	10.5

[a] Taken from Spencer et al., 1997.
[b] Determined from $k_{obs} = k_{iso}[L]/([L] + K_d) + k_{riso} + k_{chem}$.
[c] Ligand affinity after enzyme isomerization. Determined from: initial $K_d/(1 + k_{iso}/k_{riso})$.
[d] K_d values obtained from the linear fit of k_{obs} versus $[CH_2H_4PteGlu]$ using $k_{obs} = k_{on}[CH_2H_4PteGlu] + k_{off}$ and $K_d = k_{off}/k_{on}$.
[e] Enzyme isomerization is not observed (n.o.) with these mutants.
[f] Values of k_{on} and k_{off} are not directly measurable due to enzyme isomerization, so values of k_{on} and k_{off} are not applicable (n.a.).

Discussion

Clinical trials that introduce chemoprotecting genes into hematopoietic cells are aimed at protecting the recipient from the myelosuppressive side effects of chemotherapy (O'Shaughnessy et al., 1994; Hesdorffer et al., 1994; Deisseroth et al., 1996). Transfer of genes encoding MDR-1 and DHFR have advanced to clinical trials and are model systems for the study of retroviral transfer of genes that confer drug resistance (Hock and Miller, 1986; Flasshove et al., 1995;

TABLE 4

Rate constants governing inhibitor complex formation

Errors are within 10% of the reported values.

Ligand Enzyme	FdUMP		AG337	
	Wild-type ecTS	P254DecTS	Wild-type ecTS	P254DecTS
k_{on} (μM^{-1} s^{-1})	7.3	9.4	19	26
k_{off} (s^{-1})	53	230	70	550
K_d (μM)[a]	7.3	24.5	3.7	21.2

[a] Determined from $K_d = k_{off}/k_{on}$.

May et al., 1996). Because dose-limiting toxicities associated with inhibitors of TS are myelosuppression and mucositis, we have been investigating gene transfer of drug-resistant variants of TS. Previously we showed that human and ecTS can be transferred using recombinant retroviruses and that retroviral gene transfer of the human TS Y33H variant conferred resistance to FdUrd and AG337. However, the degree of resistance was only 3- to 5-fold relative to nontransduced cells (Fantz et al., 1998). It is, therefore, necessary to identify additional variants that confer greater drug resistance.

Recently, Bertino and colleagues identified drug-resistant variants of human TS using ethyl methanesulfonate to generate random mutants. Two variants were identified, D49G and G52S, that had catalytic efficiencies similar to the wild-type enzyme and that conferred resistance to AG337 and FdUrd but not to raltitrexed or BW1843U89 (Tong et al., 1998a). Resistance to raltitrexed and BW1843U89 was achieved using site-directed mutagenesis to target residues (Ile-108 and Phe-225) within the folate binding site, (Tong et al., 1998b). Although the catalytic efficiency (k_{cat}/K_m for CH_2H_4PteGlu) of the variant I108A is >200-fold lower than the wild-type enzyme, this variant conferred antifolate resistance to transfected mouse bone marrow cells. Landis and Loeb used random sequence mutagenesis to target 13 active site residues of human TS and identified a triple mutant, A197V/L198I/C199F, that had a FdUMP dissociation constant 20-fold higher than values obtained for wild-type human TS, without severely compromising catalytic efficiency (Landis and Loeb, 1998). By adapting colon tumor cell lines to increasing concentrations of FdUrd, we identified a P303L variant that conferred >20-fold resistance to both FdUrd and AG337, 4-fold resistance to raltitrexed, and 3-fold to BW1843U89 (Kitchens et al., 1999).

Because a detailed kinetic scheme has been determined for ecTS and because ecTS is, compared with human TS, intrinsically resistant to several TS inhibitors (Jackson et al., 1993; Spencer et al., 1997), the corresponding Pro to Leu substitution, along with phenylalanine, serine, glycine, and aspartic acid, were introduced at residue 254 of ecTS. Similar to human P303L, the P254L enzyme conferred resistance to FdUrd and raltitrexed. However, the degree of resistance was substantially greater (i.e., >100-fold) for the ecTS variant.

The observations that P303L in human TS is less stable than wild-type human TS, that the P254L enzyme of *E. coli* is sequestered into inclusion bodies, and that the purified Pro-254 mutant enzymes have decreased stability in vitro indicate that tertiary structural changes occur as a result of these mutations. With respect to kinetic and thermodynamic constants, the most drastic affects of mutations at residue 254 are impaired protein isomerization and diminished CH_2H_4PteGlu affinity. For instance, the affinity of the initial

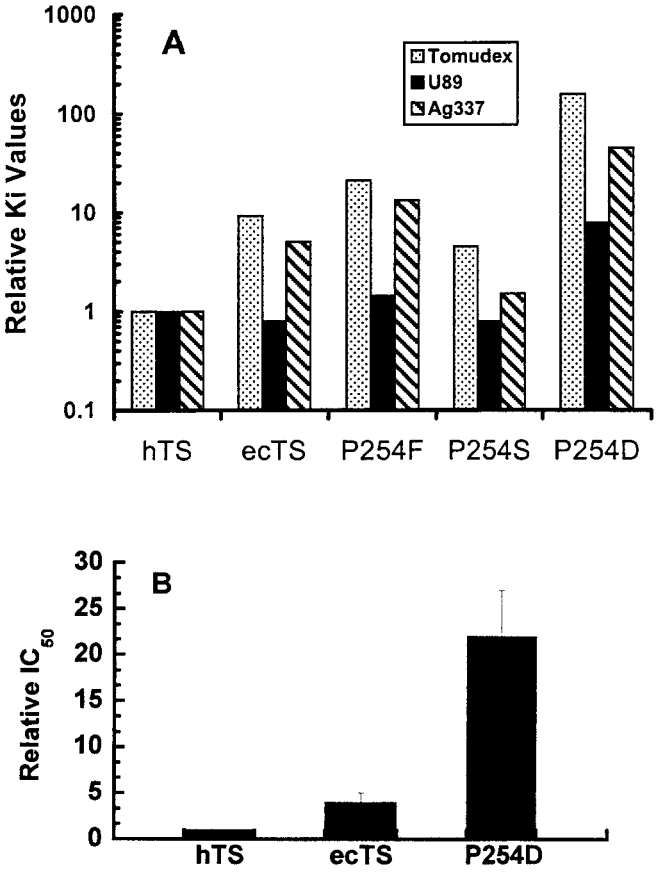

Fig. 4. A, K_i values determined for wild-type, P254F, P254S, and P254D relative to K_i values obtained for human TS; B, HaMSV retroviral vectors encoding human TS, wild-type ecTS, or P254D were transfected into RJK88.13 cells, transformants were selected in media lacking thymidine, and IC_{50} values were obtained for raltitrexed as described in Fig. 2. Error bars represent the standard deviation of the IC_{50} value obtained for wild-type ecTS or P254D relative to the IC_{50} value obtained for human TS in three individual experiments.

TABLE 5
X-ray diffraction data collection strategy

	High Resolution	Low Resolution
Wavelength	0.97930 Å	0.97930 Å
Exposure time	15 s	15 s
Detector distance	122 mm	250 mm
Omega	20	20
Delta omega	33	33
Frame width	0.4°	1.5°
Number of frames	150	40

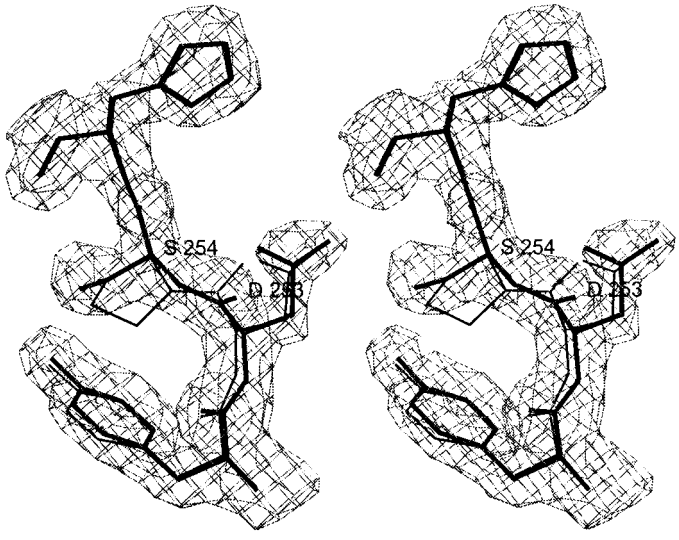

Fig. 5. Stereoview showing the peptide conformation at residue 254. The $2F_o - F_c$ electron density map is shown as basket contour at 1.4 σ level. The model of P254S TS (heavy line) is superimposed on the model of S167T TS (thin line). The peptide plane is rotated approximately 40° as shown by the position of the carbonyl group of Asp-253.

binding of CH_2H_4PteGlu forming the ternary complex is 2-fold lower for P254F, the forward isomerization rate is 7-fold slower, and the affinity after isomerization is approximately 5-fold lower compared with the wild-type enzyme. Interestingly, the P254S variant has similar steady-state values compared with the wild-type enzyme, but the isomerization reaction that is so evident for wild-type ecTS and increases the affinity of CH_2H_4PteGlu over 7-fold, is not observed with P254S. However, the affinity for CH_2H_4PteGlu, as measured by k_{off}/k_{on}, is not severely compromised for the P254S mutant (i.e., the K_d value for CH_2H_4PteGlu after protein isomerization is approximately 9 μM for wild-type ecTS and 24 μM for P254S). With respect to CH_2H_4PteGlu binding, P254D shows the most drastic differences compared with the wild-type enzyme in that values of $K_{m(CH2H4PteGlu)}$ and $K_{d(CH2H4PteGlu)}$ are substantially greater than wild-type values, whereas the values of $K_{m(dUMP)}$, $K_{d(dUMP)}$ and k_{cat} are similar to wild-type values.

Proline 254 is located 11 amino acids from the C terminus of ecTS. Crystal structures show that this residue is located at a bend that directs the C-terminal residues toward the active site. On ternary complex formation, the terminal 4–5 residues of the enzyme undergo dramatic positional changes (Montfort et al., 1990; Matthews et al., 1990). Several studies have shown that the C terminus is critical to enzyme function (Perry et al., 1993; Carreras and Santi, 1995; Spencer et al., 1997). It can be speculated that mutations at residue 254 affect ligand binding and conformational isomerization by perturbing the movement of the C-terminal residues. However, the structure of P254S suggests a different mechanism. Our modeling indicates that larger side chains at 254 must be accommodated by a movement of the side chain of Arg-48. Although located on the surface and apparently not directly involved in catalysis, ligand binding, or dimer formation, Arg-48 is a highly conserved residue. This strongly suggests that its charge is essential for the proper functioning of TS. Larger side chains at 254 will push the guanidinium moiety of Arg-48 into the solvent region, and the effect of its charge will be attenuated by the high dielectric constant of water. This hypothesis will be tested further by studying mutants of Arg-48.

In addition, the replacement of Pro-254 with serine (and presumably other amino acids) relaxes constraints on the conformation of the main chain and causes a rotation of the carbonyl plane of Asp-253 by about 40° (Fig. 5). This is accompanied by a shift of the side chain of Asp-253, which forms an ion pair with Arg-225. This change is local and does not propagate toward the C terminus. A least-squares superposition of the high resolution structures of wild-type TS and P254S does not show significant conformational changes in the 255–264 region. It should be noted, however, that the structure of ternary inhibitory complex TS/dUMP/CB3717 (Montfort et al., 1990; Protein Data Bank entry, 2tsc) in the closed conformation also shows a shift in the position of the side chain of Asp-253. There is no obvious link between the conformational change at the C terminus, which involves residues 261–264, and the shift at 253 as the residues 254–260 are not affected by the formation of the closed conformation. These observations clearly indicate some role of Pro-254 in the transition between the open and close conformations.

Variants of ecTS at residue 254 can potentially be used as modulators of TS-directed chemotherapy and may prove useful in providing proof-of-principle results in animal studies to show the applicability of TS as a chemoprotecting agent. Mutations at residue 254 cause impaired binding of TS-targeted antifolates, while maintaining catalytic efficiencies similar to the wild-type enzyme. The variant P254D conferred substantial resistance against raltitrexed and, of the variants studied, exhibited the most favorable properties for use in future gene transfer experiments. However, because the bacterial enzyme is being used, its applications may be limited due to the potential of immune responses.

References

Allay J, Persons D, Galipeau J, Riberdy J, Ashmun R, Blakley R and Sorrentino B (1998) In vivo selection of retrovirally transduced hematopoietic stem cells. *Nat Med* **4:**1136–1143.

Brunger AT, Adams PD, Clore GM, Delano WL, Gros P, Grosse-Kunstleve RW, Jiang J-S, Kuszewski J, Nilges M, Pannu NS, Read RJ, Rice LM, Simonson T and Warren GL (1998) Crystallographic & NMR system: A new software suite for macromolecular structure determination. *Acta Crystallogr Sect D Biol Crystallogr* **54:**905–921.

Carreras CW and Santi DV (1995) The catalytic mechanism and structure of thymidylate synthase. *Annu Rev Biochem* **64:**721–762.

Collaborative Computational Project, Number 4 (1994) The CCP4 suite: Programs for protein crystallography. *Acta Crystallogr Sect D Biol Crystallogr* **50:**760–763.

Davisson VJ, Sirawaraporn W and Santi DV (1989) Expression of human thymidylate synthase in *Escherichia coli*. *J Biol Chem* **264:**9145–9148.

Deisseroth AB, Kavanagh J and Champlin R (1996) Use of safety-modified retroviruses to introduce chemotherapy resistance sequences into normal hematopoietic cell for chemoprotection during the therapy of ovarian cancer: A pilot trial. *Hum Gene Ther* **7:**401–416.

Fantz C, Shaw D, Moore J and Spencer H (1998) Retroviral coexpression of thymidylate synthase and dihydrofolate reductase confers fluoropyrimidine and antifolate resistance. *Biochem Biophys Res Comm* **243:**6–12.

Flasshove M, Banerjee D, Mineishi S, Li M-X, Bertino JR and Moore MAS (1995) Ex vivo expansion and selection of human CD34 peripheral blood progenitor cells after introduction of a mutated dihydrofolate reductase cDNA via retroviral gene transfer. *Blood* **85:**566–574.

Hesdorffer C, Antman K, Bank A, Fetell M, Mears G and Begg M (1994) Human MDR gene transfer in patients with advanced cancer. *Hum Gene Ther* **5:**1151–1160.

Ho S, Hunt H, Horton R, Pullen J and Pease L (1989) Site-directed mutagenesis by overlap extension using the polymerase chain reaction. *Gene* **20:**51–59

Hock RA and Miller AD (1986) Retrovirus mediated transfer and expression of drug resistance genes in human haematopoietic progenitor cells. *Nature (Lond)* **320:**275–277.

Hyatt D, Maley F and Monfort W (1997) Use of strain in a stereo specific catalytic mechanism crystal structures of *Escherichia coli* thymidylate synthase bound to FdUMP and methylenetetrahydrofolate. *Biochemistry* **36:**4585–4594.

Jackson RC, Johnston A, Shetty B, Varney M and Webber S (1993) Molecular design of thymidylate synthase inhibitors. *Proc Am Assoc Cancer Res* **34:**566.

Kitchens M, Forsthoefel A, Barbour K, Spencer T and Berger F (1999) Mechanisms of acquired resistance to thymidylate synthase inhibitors: The role of enzyme stability. *Mol Pharmacol* **55:**1063–1070.

Koc O, Allay J, Lee K, Davis B, Reese J and Gerson S (1996) Transfer of drug resistance genes into hematopoietic progenitors to improve chemotherapy tolerance. *Semin Oncol* **23:**46–65.

Landis D and Loeb L (1998) Random sequence mutagenesis and resistance to 5-fluorouridine in human thymidylate synthase. *J Biol Chem* **273:**25809–25817.

Matthews D, Appelt K, Oatley S and Xuong N (1990) *Escherichia coli* thymidylate synthase containing bound 5-fluoro-2′-deoxyuridylate and 10-propargyl-5,8-dideazafolate. *J Mol Biol* **214:**923–936.

May C, James RI, Gunther R and McIvor RS (1996) Methotrexate dose-escalation studies in transgenic mice and marrow transplant recipients expressing drug-resistant dihydrofolate reductase activity. *J Pharmacol Exp Ther* **278:**1444–1451.

Montfort W, Perry K, Fauman E, Finer-Moore J, Maley G, Hardy L, Maley F and Stroud R (1990) Structure, multiple site binding, and segmental accommodation in thymidylate synthase on binding dUMP and an anti-folate. *Biochemistry* **29:**6964–6977.

O'Shaughnessy JA, Cowan KH, Nienhuis AW, McDonagh KG, Sorrentino BP, Dunbar CE, Chiang Y, Wilson W, Goldspiel B, Kohler D, Cottler-Fox M, Leitman S, Gottesman MM, Pastan I, Denicoff RN, Noone M and Gress R (1994) Clinical Protocol: Retroviral mediated transfer of the human multidrug resistance gene into hematopoietic stem cells during autologous transplantation after intensive chemotherapy for metastatic breast cancer. *Hum Gene Ther* **5:**891–911.

Otwinowski Z and Minor W (1997) Processing of X-ray diffraction data collected in oscillation mode. *Methods Enzymol* **307:**276–326.

Perry K, Carreras C, Chang L, Santi D and Stroud R (1993) Structures of thymidylate synthase with a C-terminal deletion: Role of the C-terminus in alignment of 2′-deoxyuridine 5′-monophosphate and 5,10-methylenetetrahydrofolate. *Biochemistry* **32:**7116–7125.

Reilly RT, Barbour KW, Dunlap RB and Berger FG (1995) Biphasic binding of 5-fluoro-2′-deoxyuridylate to human thymidylate synthase. *Mol Pharmacol* **48:**72–79.

Sack JS and Quiocho FA (1997) CHAIN: A crystallographic modeling program. *Methods Enzymol* **277:**158–173.
Sorrentino BP, Brandt SJ, Bodine D, Gottesman M, Pastan I, Cline A and Nienhuis AW (1992) Selection of drug-resistant bone marrow cells in vivo after retroviral transfer of human MDR. *Science (Wash DC)* **257:**99–103.
Spencer HT, Sleep SH, Rehg JE, Blakley RL and Sorrentino BP (1996) A gene transfer strategy for making bone marrow cells resistant to trimetrexate. *Blood* **87:**2579–2587.
Spencer HT, Villafranca JE and Appleman JR (1997) Kinetic scheme for thymidylate synthase form *Escherichia coli*: Determination from measurements of ligand binding, primary and secondary isotopes effects, and presteady-state catalysis. *Biochemistry* **36:**4212–4222.
Tong Y, Liu-Chen X, Ercikan-Abali E, Capiaux G, Zhao S, Banergee D and Bertino J (1998a) Isolation and characterization of thymitaq (AG337) and 5-fluoro-2-deoxyuridylate-resistant mutants of human thymidylate synthase from ethylmethanesulfonate-exposed human sarcoma HT1080 cells. *J Biol Chem* **273:**11611–11618.
Tong Y, Liu-Chen X, Ercikan-Abali E, Zhao S, Banergee D, Maley F and Bertino J (1998b) Probing the folate-binding site of human thymidylate synthase by site-directed mutagenesis. *J Biol Chem* **273:**31209–31214.
Touroutoglou N and Pazdur R (1996) Thymidylate synthase inhibitors. *Clin Cancer Res* **2:**227–243.

Send reprint requests to: H. Trent Spencer, Department of Biological Sciences, University of South Carolina, Columbia, SC 29208. E-mail: spencer@psc.sc.edu